Final Report

on

DEVELOPMENT OF PIEZOELECTRIC SKIN-FRICTION-FORCE VECTOR TRANSDUCER FOR A HYPERSONIC WIND TUNNEL

Submitted to

NATIONAL AERONAUTICS AND SPACE ADMINISTRATION

Prepared by

Dr. Seun K. Kahng

Assistant Professor of Electrical Engineering

University of Oklahoma

Submitted by

UNIVERSITY OF OKLAHOMA RESEARCH INSTITUTE

1808 Newton Drive

Norman, Oklahoma 73069

Final Report

on

DEVELOPMENT OF PIEZOELECTRIC SKIN-FRICTION-FORCE-VECTOR TRANSDUCER FOR A HYPERSONIC WIND TUNNEL

Grant NGR 37-003-045

Submitted to

NATIONAL AERONAUTICS AND SPACE ADMINISTRATION

Prepared by

Dr. Seun K. Kahng
Assistant Professor of Electrical Engineering
University of Oklahoma

Submitted by

UNIVERSITY OF OKLAHOMA RESEARCH INSTITUTE
1808 Newton Drive
Norman, Oklahoma 73069

May, 1972

PREFACE

This final report describes the development by the University of Oklahoma Research Institute of a Piezoelectric Skin-Friction-Force-Vector Transcuder under grant NGR 37-003-045 to NASA/Langley Research Center, Hampton, Virginia. The grant period was from August 1, 1969, until November 30, 1971. Transducers were developed under this grant and delivered to Mr. D.A. Smith of IRD, LRC, NASA.

ABSTRACT

A new type of surface shear force transducer for use in impulse type hypersonic tunnels is described. The design of the transducer is based upon the design requirements of the transducer specified in the initial proposal submitted.

Sensors are constructed of lead zirconate titanate composition piezoelectric ceramic materials. The diameter of the sensing diaphragm is 0.75 inches and overall transducer dimensions are 1.0 inch diameter and 0.625 inch height. Analysis of the transducer is made to help design criteria and fabrication techniques. Discussions on design and fabrication techniques are presented as well as performance of transducers delivered.

TABLE OF CONTENTS

LIST OF FIGURES

LIST OF TABLES

INTRODUCTION

The work reported deals with a specific transducer, a two component piezoelectric surface shear force transducer. The transducer is intended to make measurements of local surface shear force on an aerodynamic body in an impulse type hypersonic tunnel.

The transducing element has an H-beam configuration composed of three piezoelectric ceramic beams. Two H-configuration transducing elements are contained in the transducer, one as the surface shear force sensing element and the other as an acceleration compensating element which is isolated from the surface shear force. A surface shear force exerted on the transducer is converted into a proportional charge. A component of the surface shear force is measured by the center beam of the H-configurgation transducing element and a corresponding perpendicular component of the force is measured by the side beams of the transducing element.

Design specifications for the transducer are as follows:

Skin-friction-range	0.0005 to 0.01 psi(flow direction) 0.00005 to 0.001 psi (perpendicular to flow direction)
Rise time	2 milliseconds or less
Test duration	20 to 100 milliseconds
Temperature range	75°F to 100°F
Relative sensitivity of skin friction to acceleration in sensitive axes	100:1
Maximum normal overpressure	20 psi
Relative sensitivity of skin friction to normal pressure	300:1
Cross coupling factor	100:1
Maximum acceleration	50 g's
Physical dimensions	less than 1 in OD x 3/4 in height, approximately 1/2 in sensing diaphragm diameter

THEORY

The transducing element employs a piezoelectric ceramic Bimorph* which has the capacity for handling larger motions and smaller forces than a single piezoelectric plate. The Bimorph consists of two plates of lead-zirconate-titanate ceramics (PZT-5H) which are polycrystalline in nature such that the piezoelectric behavior is induced by a polarizing treatment. PZT-5H has the desirable characteristics of low temperature dependence and a high piezoelectric constant. The two ceramic elements are separated by a conductive center vane which adds rigidity to the beam, and the outside faces are coated with a nickel electrode as shown in Figure 1.

In this manner any voltage applied to the Bimorph causes the plates to deform in opposite directions; and conversely any bending of the elements will develop a corresponding voltage between the electrodes.

The method used to obtain the corresponding voltage output for a step input force is to analyze the electro-mechanical equivalent circuit of the piezoelectric beam.

The electro-mechanical representation of a piezoelectric element is given[1] in Figure 2, where M is the effective mass of the beam, C_m is the mechanical compliance of the beam, and C_e is the electrostatic capacitance of the beam.

Considering a unit step force and referring "C_m" to the primary side the new representation is given in Figure 3.

*Bimorph is a trade name by Clevite Corporation for a flexing type piezoelectric ceramic element.

[1] Warren P. Mason, Proceedings of the IRE, "Uses of Ultrasonics in Radio, Radar, and Sonar Systems," Vol. 50, No. 5 (May, 1962), pp. 1374-1392.

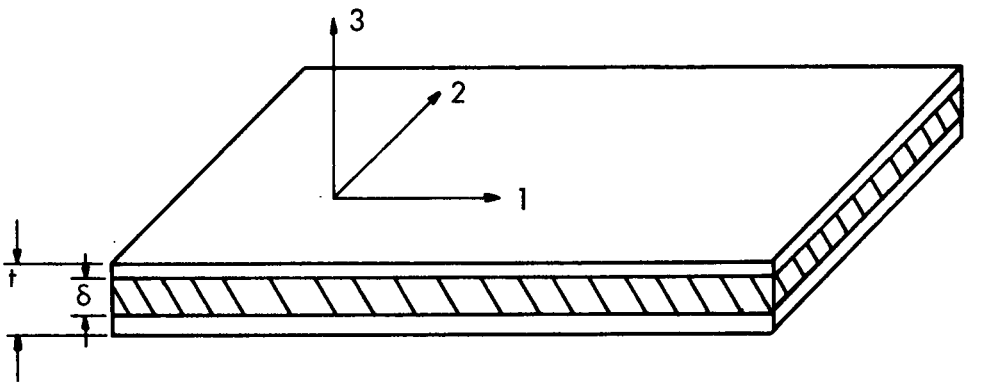

Figure 1. Cross-Section of a PZT Element

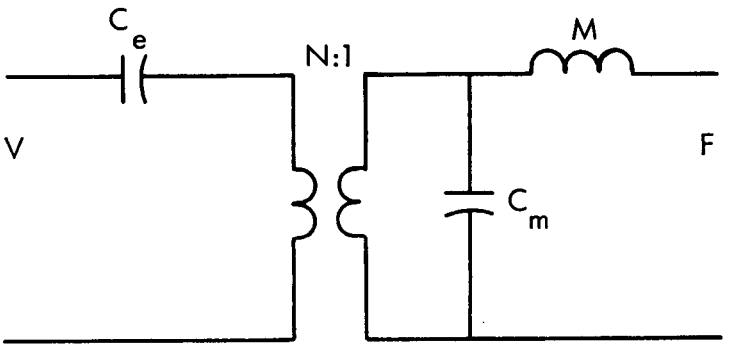

Figure 2. Electromechanical Equivalent Circuit

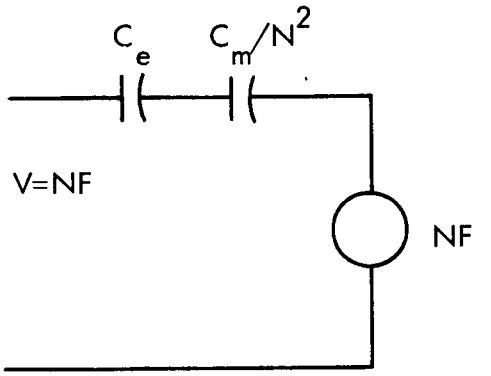

Figure 3. Transformed Equivalent Circuit

Using the relationships between the Force and the Charge it is readily seen that

$$Q = \frac{NC_e d}{C_m + N^2 C_e} \tag{1}$$

where N is the voltage to force ratio[1] and d is the deflection. In other words the charge output is directly related to the product of concentrated applied force and the electrostatic capacitance across the beam and a corresponding ratio between the open circuit voltage and applied force.

An H-beam configuration was selected for the two component sensing elements. Figure 4 shows the two side beams were aligned such that any force acting perpendicular to their longitudinal axis corresponded to the x-direction, and any force perpendicular to the longitudinal axis of the center beam corresponded to the y-direction.

The charge output for the y-axis is taken directly off the center beam, and the charge output for the x-axis is taken across the two side beams. However, the two side beams are connected in series such that the measured charge is actually the charge produced on one beam. The series connection is necessary because when a force is applied in the y-direction, the two side beams will deform due to the moment generated by the force acting perpendicular to the center beam. However, as shown in Figure 4 the side beams will deform in such a manner that the charge developed across them will cancel due to the series connection.

With the understanding of the H-beam configuration and the PZT elements, a method of analyzing the expected charge output is presented.

When a PZT beam is deflected, a positive and negative charge is produced on the beam due to the compression and tension on the beam. As it is shown in Figure 5, it is possible for both sides of the beam to experience compression and tension which

[1] Carmen Germano, Useful Relationships for Rectangular Ceramic Bender Bimorphs (Bedford, Ohio: Piezoelectric Div., Clevite Paper TP-223).

results in a charge cancellation. To avoid this, the electrodes on the surfaces of the beams are separated at the inflection points and the charge is measured over the center electrode portion of the beam.

The analysis of the charge output proceeds in the following manner. Each side beam will experience half of the total force applied in the x-direction and half of this force is experienced by each half of the single beam. The side beam consists of two capacitors in series with equal charge on both capacitors. The total voltage developed across the beam is denoted by V_T, and the voltage across each capacitor is denoted by V as is shown in Figure 6. Therefore, the charge produced on the beam is

$$Q = C_{e1}V = C_{e2}V, \tag{2}$$

and the total capacitance

$$C_{eT} = C_{e1}\, C_{e2}/(C_{e1} + C_{e2}) = C_{e1}/2 \tag{3}$$

where

$$C_{e1} = \epsilon\epsilon_o \frac{wla}{t/2\,(1-\delta/t)} \tag{4}$$

and $(1-\delta/t)$ is the thickness of the two PZT plates less the thickness of the center vane. By definition for piezoelectric constants[1]

$$g_{31} = \frac{\text{field developed in 3 direction}}{\text{stress applied in 1 direction}} \left[\frac{\text{Volts/meter}}{\text{Newtons/meter}^2} \right]$$

where the 3 and 1 directions are designated in Figure 3.

---

[1] Clevite Corporation Piezoelectric Division., Piezoelectric Technology Data for Designers (Clevite Corporation Piezoelectric Division, 1965), p. 14.

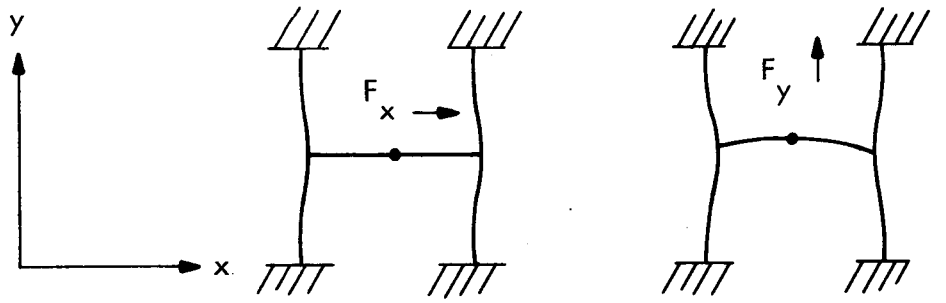

Figure 4. H-Beam Loading

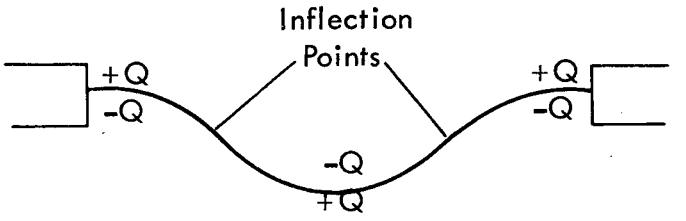

Figure 5. PZT Beam Deflection

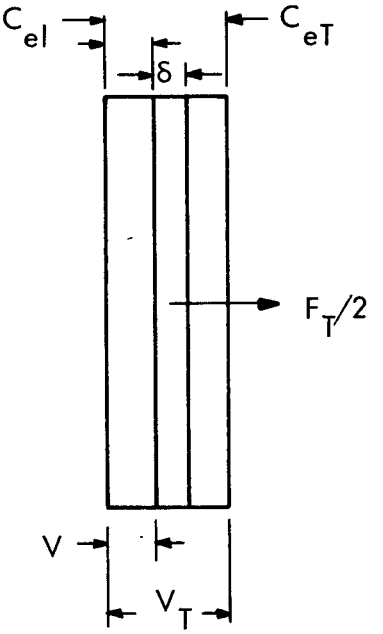

Figure 6. PZT Beam

The electric field developed across the beam is

$$E = \frac{V_T}{t(1-\delta/t)} \tag{5}$$

and the applied stress is

$$S = Moy/I \tag{6}$$

where the bending moment is

$$Mo = \frac{(F_T/2)la}{8} \tag{7}$$

$$S_{max} = 1/8 \frac{(F_T/2)la(t/2)}{wt^3/12} \tag{8}$$

and the average stress is

$$S_{avg} = 3/16 \frac{F_T\, la}{wt^2} \quad . \tag{9}$$

Substituting for E and S_{avg}, g_{31} is found to be

$$g_{31} = \frac{V_T/(1-\delta/t)}{3/16\ (F_T la/wt)} \quad . \tag{10}$$

From this equation the transducer ratio is

$$N = V_T/F_T \tag{11}$$

and substituting for V_T and F_T

$$N = (3/16)\ g_{31}\ (la/wt)\ (1-\delta/t) \quad . \tag{12}$$

The deflection, d, between the inflection point and the center of the side beam is given by[1]

[1] Raymond J. Roark, Formulas for Stress and Strain (McGraw-Hill Book Co., Inc., 1965).

$$d = \frac{F_T/2}{EI} \int_{xo}^{la/2} ((x^2/4) - (la\ x/8))dx \qquad (13)$$

such that

$$d = \frac{F_T/2}{EI} \left[\frac{la^3}{192} + \frac{X_o^3}{12} - \frac{X_o^2\ la}{16} \right] \qquad (13)$$

where X_o is the length of the beam from the inflection point to the end of the beam.

The compliance for the side beam is given by

$$C_m = Y_{max}/Force \qquad (15)$$

hence

$$C_m = la^3/192EI \quad . \qquad (16)$$

Therefore, the total charge produced across the side beam is

$$Q_T = \frac{\epsilon\epsilon_o 18 g_{31} F_T \left[\frac{la^3}{192} + \frac{X_o^3}{12} - \frac{X_o^2\ la}{16} \right]}{t^2 la} \quad . \qquad (17)$$

The N^2C_e term from equation 1 has been neglected since it is negligible as compared to C_m.

The equation for the charge produced by the center beam proceeds as follows. The capacitance and electric field are the same as the side beam case, but the applied stress is different.

The applied stress is

$$S = \frac{Moy}{I} \quad \text{where} \quad Mo = \frac{F_T\ lc^2\ Eala}{8\ lcEala + Eclala} \qquad (18)$$

and

$$E_a I_a = E_c I_c \text{ such that } M_o = \frac{F_T lc^2}{8\ lc + la} \quad . \qquad (19)$$

Therefore

$$S_{avg} = \frac{3}{wt^2} \quad \frac{F_T lc^2}{8lc + la} \tag{20}$$

$$g_{31} = \frac{V_T/t(1-\delta/t)}{3F_T\, lc^2} \Big/ \frac{}{(8lc + la)wt^2} \tag{21}$$

and

$$N = \frac{3\, g_{31}\, lc^2\, (1-\delta/t)}{(8lc + la)\, wt} \quad . \tag{22}$$

The deflection for the center beam is

$$d = \frac{F_T lc^3}{8EI} \quad \left[\frac{21c+1a}{6(81c+1a)}\right] - \frac{F_T}{2EI} \quad \left[\frac{lc^2 X_o}{8} - \frac{X_o^3}{6} - \frac{lc^3 X_o - lc^2 X_o^2}{81c+1a}\right] \tag{23}$$

and the compliance is

$$C_m = \frac{F_T lc^2}{8EI} \quad \frac{21c^2+1a1c}{6(81c+1a)} \tag{24}$$

Finally, the total charge for the center beam is

$$Q_T = \frac{K\left[\frac{F_T lc^3}{8EI} \quad \frac{21c+1a}{6(81c+1a)} - \frac{F_T}{2EI}\left[\frac{lc^2 X_o}{8} - \frac{X_o^3}{6} - \frac{lc^3 X_o - lc^2 X_o}{81c+1a}\right]\right]}{t^2\left[21c^2 + 1a1c\right]} \tag{25}$$

where $K = 18 g_{31} \epsilon \epsilon_o lc^3$.

CONSTRUCTION

Construction of several of the transducer prototypes was a slow and delicate process due to the delicate PZT elements and the small dimensions of the transducer, 0.500 inches in diameter and 0.625 inches in height.

The length, width, and thickness of the PZT-5H beams were 0.400 inches, 0.050 inches, and 0.020 inches with a center vane thickness of 0.0066 inches. At the beam inflection points the electrodes on the surface were separated such that at least 10^{12} Ω resistance existed between the two separated portions. Approximately 0.040 inches on each end of the side beams was constrained by the epoxy holding the H-beam to the housing. The resulting effective length of the side beams was 0.320 inches with the inflection points occurring at 0.080 inches from the effective end of the beam. In turn the ends of the center beam were constrained by the epoxy attaching it to the centers of the two side beams. The effective length of the center beam was 0.412 inches with the inflection points occurring at 0.115 inches from the end of the beam.

Two H-beam configurations, a transducing and compensating configuration, were placed in the transducer housing such that their x and y axis coincided with the compensating configuration placed directly below the transducing configuration. They were electrically wired together such that any force experienced by both of the configurations would produce equal charges, but the wiring caused cancellation of the charges. The charge cancellation is necessary to eliminate any spurious signal due to external vibrations experienced by the transducer. A cutaway view of the transducer is shown in Figure 7. The actual sensing element was mechanically coupled to a diaphragm which was subjected to the surface shear force. The circular diaphragm is 0.750 inches in diameter and had a thickness of 0.010 inches. A smaller perforated disk which has a heat resistive path connected the sensing diaphragm to the center of the H-beam configuration. The compensating configuration was not exposed to any surface shear force. A counterbalance weight equalling the combined weight of the sensing diaphragm and the perforated disk was attached to the center of the compensating H-beam configuration. To

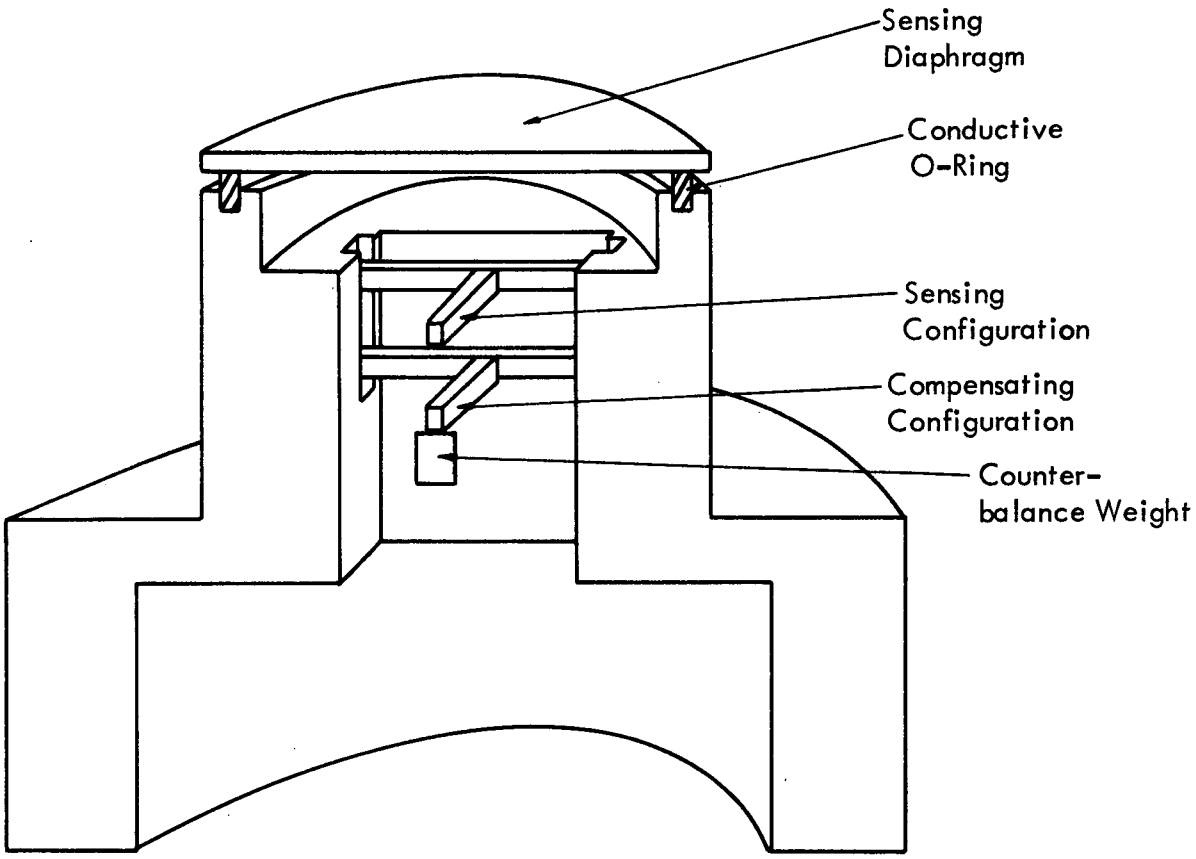

Figure 7. Cutaway View of the Surface Shear Force Transducer

prevent any charge accumulation on the sensing diaphragm which affects the charge on the PZT elements, the sensing diaphragm was electrically grounded to the transducer housing by a conductive O-ring which fit between the housing and diaphragm.

A metal with a low thermal expansion coefficient, invar, was used to fabricate the transducer housing, circular diaphragm, and counterbalance weight. A metal with a low thermal expansion coefficient is needed to lessen the effect of erroneous signals or spurious noise introduced by the thermal expansion of the transducer housing.

The piezoelectric beams were very susceptible to contaminations, such as dust and moisture from the environment and dirt and oil from handling. The contamination causes a decrease in the beam resistance which lowers the time constant. This is directly related to D.C. characteristics by allowing the charge leakage rate to increase. Therefore, it was necessary to work in a clean atmosphere and subject the parts to cleaning: acetone, ethyl alcohol, and distilled water, before and after they were placed in the transducer housing.

EXPERIMENTAL PROCEDURE

The method of calibrating the surface shear force transducer was to apply a step input force to the surface of the diaphragm and measure the corresponding charge output. The charge output was then transformed to a voltage which was amplified and recorded.

The step input force was simulated by releasing a known weight which was suspended from the center of the sensing diaphragm. When the weight is in suspension, the beams deflect from their normal rest positions producing a charge on the electrodes. Before the weight is released, this charge is drained off the beam allowing the beam to produce a new charge when it returns to its normal position.

The experimental setup was mounted on a vibrational isolation table which dampened any vibration inherent in the laboratory. Any vibration produced by the surroundings will interfere with the low range sensitivity measurements. The transducer was mounted on a rotational indexing table which allowed the transducer to be rotated 360°. The indexing table and transducer were both situated such that their axis of rotation was horizontal and in this manner, the weight suspended from the center of the diaphragm was released by striking it with a lever arm attached to a relay.

The transducer was either loaded parallel to the x or y axis corresponding to a force on the side beams or center beam respectively. Alignment holes on the transducer were situated such that when the transducer was mounted on the rectangular mounting bracket on the indexing table the edge of the beams were parallel to the edges of the rectangular bracket. A cathatometer was used to align the axis of the transducer so that edges of the bracket were exactly horizontal and vertical insuring the force produced by the suspended weight was only on one of the axes.

There were three specific experiments run on the transducer, a first order interaction test, a second order interaction test, and a temperature dependence test. In all

three experiments the transducer was loaded with seven different weights; 20, 15, 10, 5, 0.5, 0.1, and 0.02 mpsi; and these weights were loaded along the positive and negative direction of each axis by rotating the transducer 180°. The first order interaction test involved loading the transducer along one axis and monitoring both axes for the charge produced along the loaded axis and any charge produced along the other axis due to the interaction between the beams. For the second order interaction test, an auxiliary stationary force of 5 milli psi was applied to the axis perpendicular to the loading axis. The cathatometer was used to align the second force, and as before both axes were monitored for any interaction between them. As shown in Figure 8 the transducer is temperature dependent due to the temperature dependence of the dielectric constant ϵ_{33} and the piezoelectric constant g_{31}. For the temperature dependence test the transducer was placed in an oven and a thermocouple was placed inside the transducer cavity such that as little temperature gradient as possible existed between the inside and outside of the transducer housing. The transducer was loaded as in the first order interaction test, but the ambient temperature was set at 50°C and 70°C for two separate experiments.

The problem in precisely measuring the charge outputs of the piezoelectric transducer is that the step input force maintains a DC level for only a few milliseconds. Therefore, a system must be employed which has a rise time at least as fast as the transducer and which is capable of displaying the signal. The method employed was to subtract a known signal level from the measured output signal, amplify the difference, and record this difference on an oscillograph recorder. Thus, the unknown signal is equal to the sum of the known signal and the recorded difference.

However, there are still several procedures to be made to insure an accurate measurement of the transducer's charge output. First, a difficulty arises in synchronizing the release of the weight with the initiation of the cancelling signal. From Figure 9 it is seen that the closing of the relay initiates the cancelling signal. The weight may be lowered or raised by the indexing table such that the weight is struck when the relay contacts close.

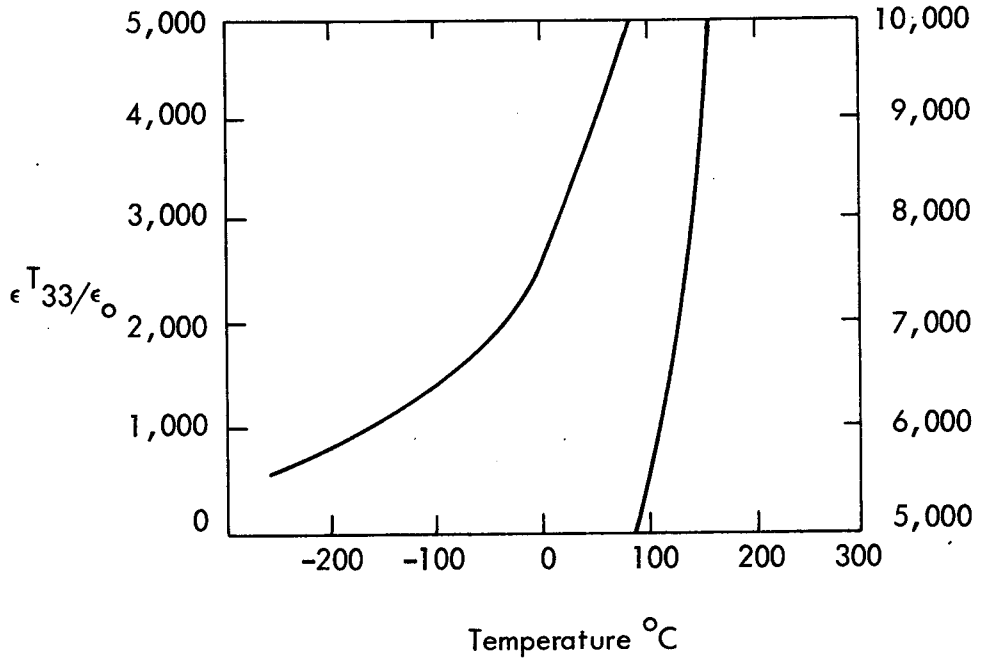

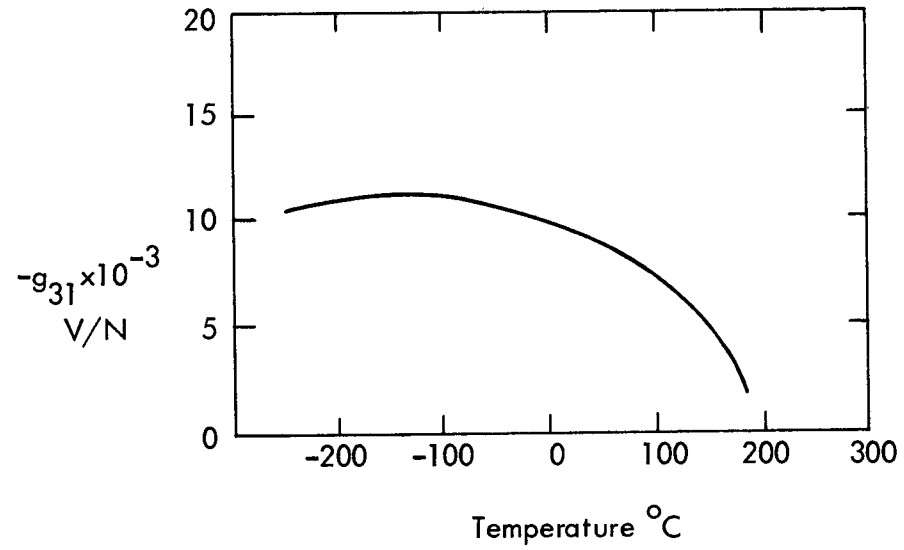

Figure 8. Dielectric Constant and Piezoelectric Constant Versus Temperature

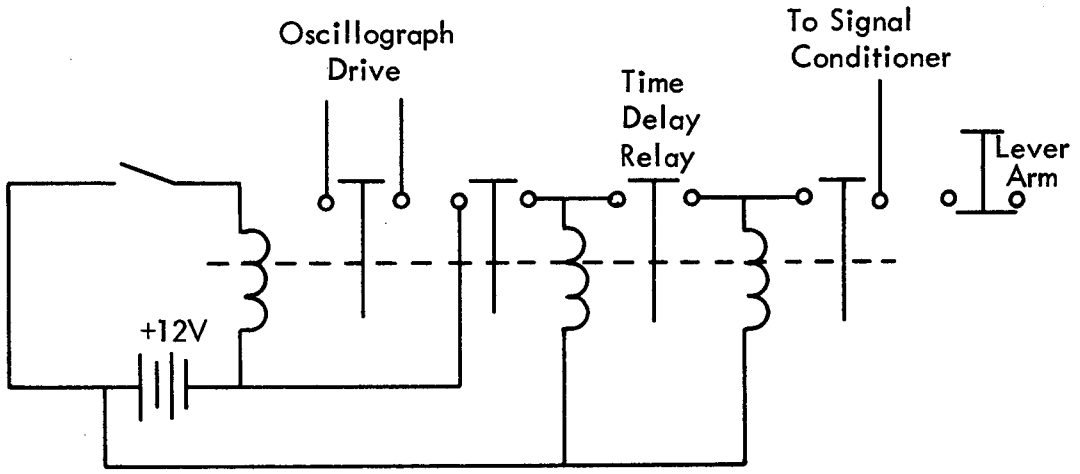

Figure 9. Relay Configuration

Secondly, when using small weights below 5 mpsi, the difference signal is hard to extract because the low level output is imbedded in the inherent oscillation imposed on the signal which becomes very pronounced on the oscillograph paper. The inherent oscillation is due to the mechanical resonance of the transducer which for low level measurements predominates when the D.C. portion of the signal has been cancelled out. Therefore it is necessary to use extreme caution in taking readings for the low levels. Thirdly, if the piezoelectric beams or the leads within the transducer have been contaminated then the rate of charge leakage increases due to the decrease in the time constant. This can be checked easily by observing the transducer under a no load condition. To avoid this problem the beams must be cleaned and protected from any contamination. Fourthly, as mentioned before, the transducer is temperature dependent and the ambient temperature should be held constant to eliminate any incorrect data. Although the rise times may be equal, the shapes of the transient responses cannot be perfectly matched, and a deviation between the actual signal and the cancelling signal exists. Therefore, when reading the difference signal at least 1 msec. was allowed from the time of the initial deviation to eliminate any transient response discrepancies. These were the primary problems encountered in obtaining data, but they presented no difficulty since they were diagnosed in advance.

Before fully describing the data acquisition system, a brief description will be given of the equipment. A charge amplifier was used for converting the transducer's charge output to a voltage signal. As shown in Figure 10 the signal conditioner which follows the charge amplifier consists of four sections; the switching circuits, the oscilloscope trigger pulse, the cancelling signal circuits, and the differential amplifiers. There are two switching circuits on which, when an input level is supplied, a +12 volt level exists on one output and a -12 volt level exists on the other output, and an RC circuit uses the +12 volt output to generate a triggering signal for the storage oscilloscope. The cancelling signal RC circuits can be connected to either of the switching circuit's outputs making it possible to match a positive or negative signal. The amplitudes can be varied from 0 to 12 volts and the rise time from several microseconds to approximately 3 milliseconds. The cancelling signals are then connected

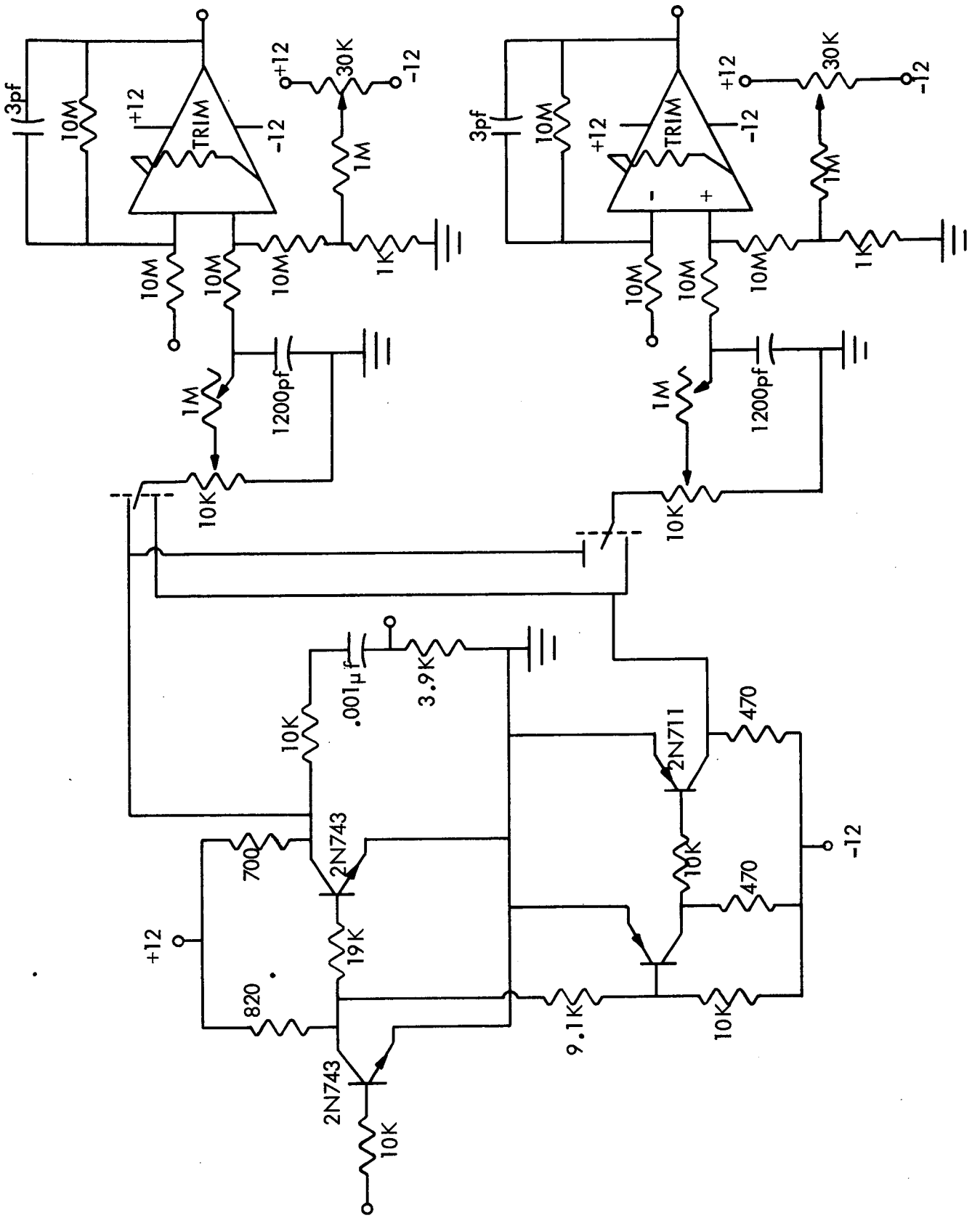

Figure 10. Signal Conditioner

to the differential amplifiers which are constructed from two operational amplifiers. Following the signal conditioner are a DC Amplifier and an oscillograph recorder which are used to amplify the difference signal and finally to record it. A storage oscilloscope was used to display the output signal for the precalibration tests and a digital voltmeter measured the cancelling signal.

The relay configuration in Figure 9 consists of three relays whose purposes are allowing 200 msec in advance for the oscillograph paper driver to reach full speed and supplying an input signal to the signal conditioner. The rise time of the lever arm which releases the suspended weight is 0.5 msec, and once the weight has been released the transducer produces a charge output on its x and y axis. The block diagram in Figure 11 shows these outputs are applied to the charge amplifier and converted to voltage signals which are dependent upon the transducer sensitivity and range settings of the amplifier. The charge amplifier outputs are fed to the signal conditioner where they are applied to the inverting input of the differential amplifiers. On the noninverting inputs a signal is applied which has been matched, as closely as possible, to the charge amplifier outputs.

In this manner the rise time and amplitude are matched as they appear on the oscilloscope. The differential output is fed into the D.C. amplifier which feeds its output to the oscillograph. Therefore, by measuring the cancelling signal voltage which is a constant D.C. level with the digital voltmeter, and adding the deflection which must be divided by the sensitivity of the oscillograph in inches per volt and the amplifier gain, the transducer voltage level is obtained.

A computer was used for calculating the charge output and sensitivity for each axis by evaluating the following equation:

$$S = \frac{VcTDR}{GS \cdot G(PSI)} \tag{26}$$

where S is the sensitivity, Vc the cancelling voltage, T the transducer sensitivity setting, D the deflection on the oscillograph paper, R the range setting, GS the

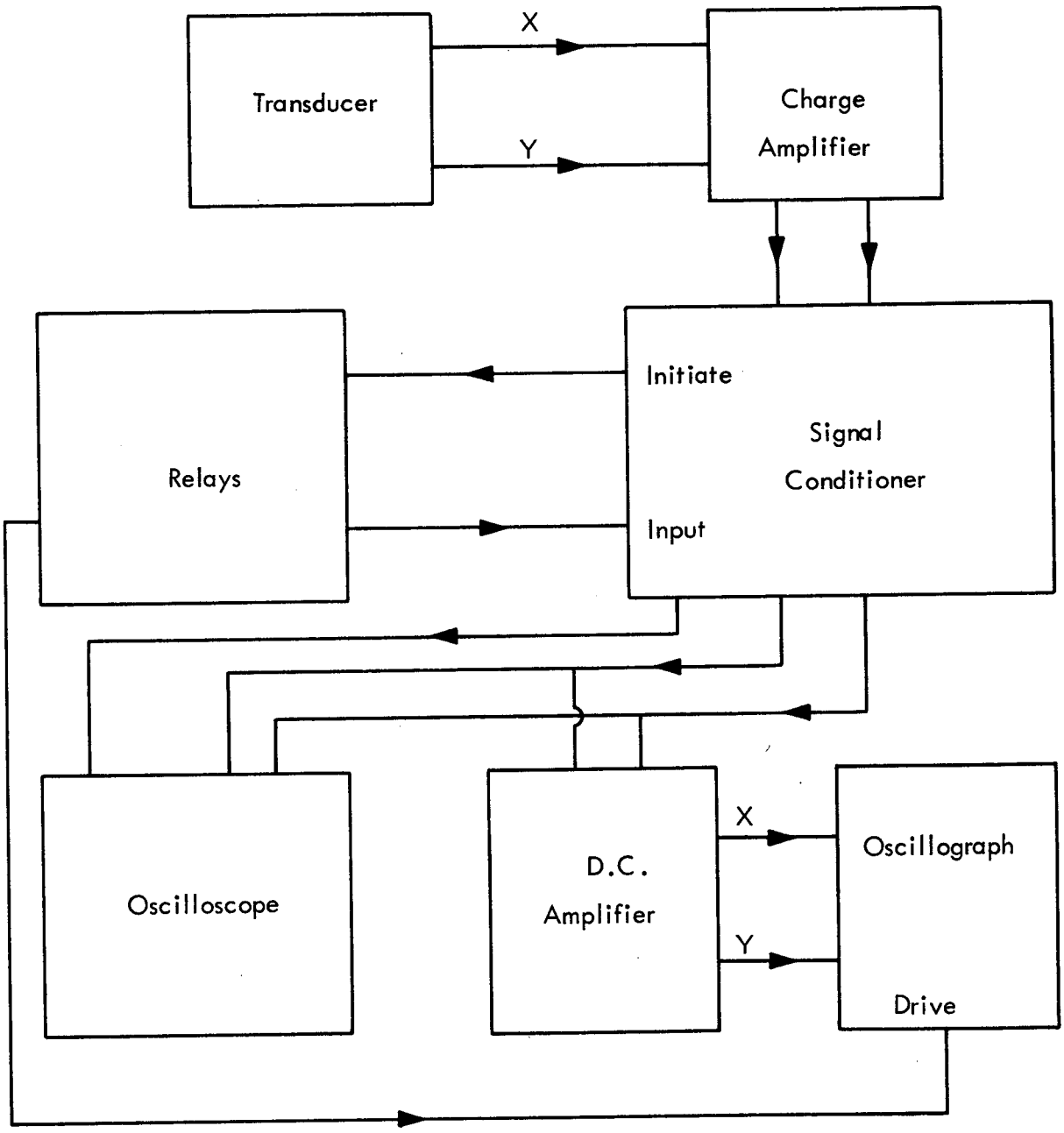

Figure 11. Calibration Setup

sensitivity of the oscillograph galvanometer, G the amplifier gain, and PSI the applied force.

The method used has the capability of accurately measuring the charge output of the piezoelectric transducer. There are certainly other methods which could have been employed such as a sampling device connected to an analog to digital converter which stores its information on tape, but the method described here is adequate for present purposes.

DISCUSSION OF RESULTS

Table I gives the frequencies and spring constants, K, for the respective axes. The spring constant is obtained by using 0.900 grams for the total mass of the diaphragm and H-beam configuration and solving for K in the following equation:

$$f = \frac{1}{2\pi} \sqrt{Kg/m} \qquad (27)$$

where f is the frequency and g is the acceleration of gravity.

Table II shows the results of the transducer sensitivity measurements as compared to the calculated sensitivity. The calibrated results are the average sensitivity measurements of each transducer. As is seen, transducer #1 approaches the predicted values but the others are of the order of 2/3, 1/2, and 1/3 of the calculated results. Referring to Table I it is seen that the increase frequency for each transducer parellels the decrease in sensitivity. This is due to the epoxy spreading onto the PZT beams which increases the spring constant and decreases the deflection of the beam. The reason it is due to the spring constant rather than a change in mass is that for deviation of 0.100 grams from 0.900 grams the frequency varied by 6.1% which is not enough to account for the large variations in frequency or sensitivity.

Table III shows the nonlinearity of each transducer and is expressed as the absolute value of the percent of deviation from the full scale reading. A plot of charge versus load is shown in Figure 12.

The first and second order interactions are given in Table IV. The first order interaction is the percent in reading deviation of the loaded axis as compared to the same axis when it is not loaded. The second order interaction of the percent in reading deviation from the loaded axis as compared to the same loaded axis when an auxillary weight is placed on the off axis.

TABLE I

NATURAL FREQUENCIES* Hz

Transducer	y(H_z) Direction	Ky lbs/in	x(H_z) Direction	Kx lbs/in
#1	1,780	605	3,600	2,460
#2	3,333	2,100	5,000	4,750
#3	4,150	3,280	5,000	4,750
#4	4,200	3,300	5,800	5,300
#5	5,000	4,750	7,500	10,500
Calculated	2,280	990	4,730	4,250

*The measured frequencies were distorted sinusoids (as shown below) due to the contact between the conductive O-ring and the sensing diaphragm.

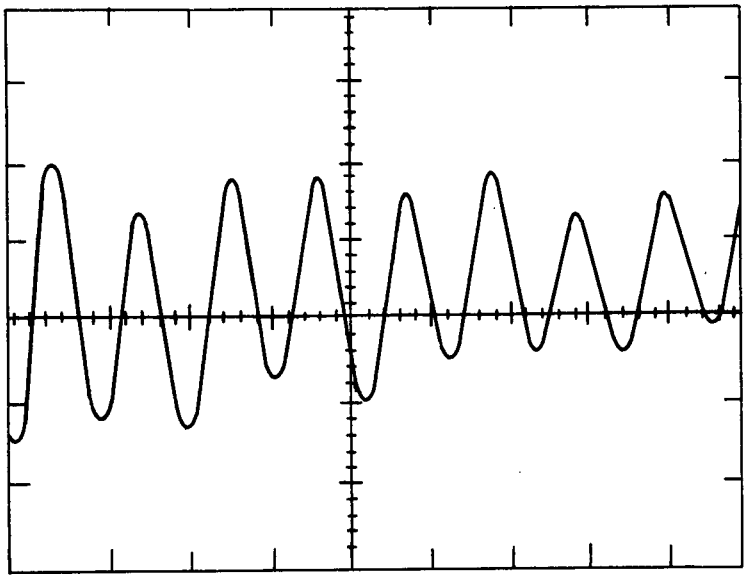

This is a diagram of a photograph of the resonance frequency at the y-axis approximately 3 msec after the step input force was applied. The horizontal scale is 0.5 msec/cm and the vertical scale is 0.1 V/cm. The same distortion is present on the x-axis output but was not as pronounced as on the y-axis output.

TABLE II

SENSITIVITIES

Direction	Measured Results (Pc/mpsi)					
First Order	#1	#2	#3	#4	#5	Calculated
x Direction	6,103.67	4,109.3	3,343.0	2,812	2,335.25	6,383.2
y Direction	23,182.	6,872.8	4,135.6	3,733	3,247.4	28,956.
Second Order						
x Direction	6,038.4	3,998.0	3,377.7	2,909	2,226.8	6,383.2
y Direction	22,998.	6,973.3	3,790.2	3,799	2,664.64	28,956.

TABLE III

NONLINEARITIES

Direction	Transducer Results				
First Order	#1	#2	#3	#4	#5
x Direction	0	0	0	0	4.25
y Direction	0.25	5.84	6	4.6	3.5
Second Order					
x Direction	0	3.68	4.4	4.1	6.3
y Direction	0.25	3.18	3.85	3.7	5.1

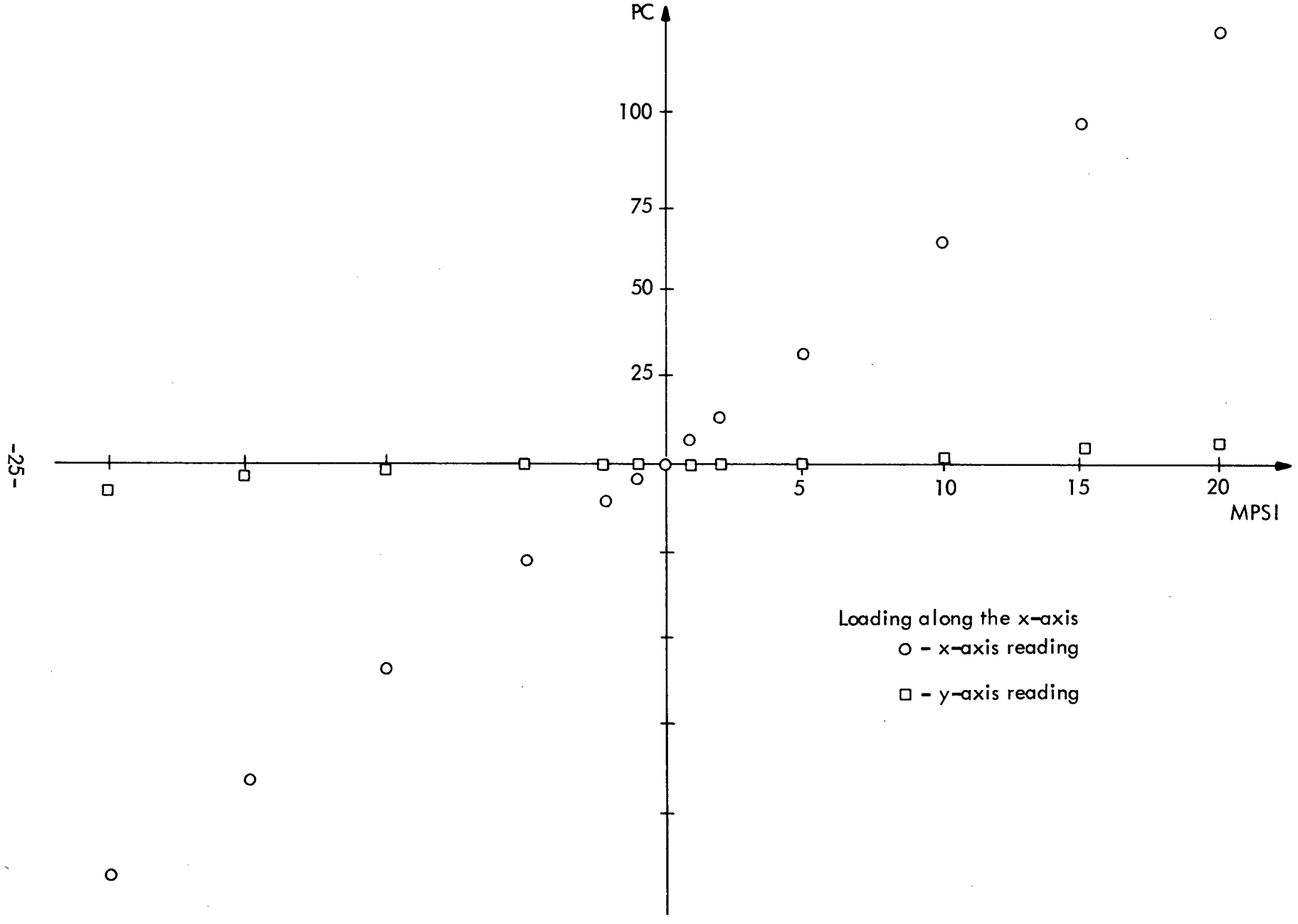

Figure 12. Charge vs. Force

TABLE IV

FIRST AND SECOND ORDER INTERACTIONS

Direction	Results				
First Order Interaction	#1	#2	#3	#4	#5
x Direction	0.39	3.84	1.68	1.56	1.27
y Direction	0.323	0.42	2.13	2.00	1.9
Second Order Interaction					
x Direction	0.122	2.38	1.1	1.00	3.54
y Direction	0.198	7.5	1.87	1.50	3.95

The typical temperature dependence of a transducer is given in Table V. The calculated results were obtained by choosing the corresponding values of g_{31} and ϵ^{T}_{33} at the appropriate temperature. The transducer closely matches calculated results at room temperature, but as the temperature increases and the expected sensitivity increases, the measured sensitivity does not increase in proportionate amount. There would appear to be other temperature factors which have not been taken into account such as the temperature gradient which exists between the inside and outside of the transducer and stresses and strains introduced by the increase in temperature. Also, shown in the table is the percent of deviation from the 25° reading.

The overall performance data are given in Table VI.

TABLE V

TEMPERATURE DEPENDENCE

Direction	(Pc/mpsi) Sensivity*	% of 25°C	Calculated	% of 25°C	Temperature
x	6,103.67	0	6,383.2	0	25°C
	6,401.4	4.8	7,181.1	12.5	50°C
	6,491.7	6.4	7,843.4	23	70°C
y	25,841	0	28,956	0	25°C
	27,204	5.3	32,576	12.5	50°C
	27,800	7.5	35,580	23	70°C

*Average Sensitivity

TABLE VI

PERFORMANCE DATA

Transducer	1	2	3	4	5
Type of Ceramics	PZT-5H	PZT-5H	PZT-5H	PZT-5H	PZT-5H
Materials	Invar	Invar	Invar	Invar	Invar
Sensing Area (in^2)	0.442	0.442	0.442	0.442	0.442
Sensitivity in x-direction (pc/psi)	6,100	4,100	3,300	2,800	2,300
Sensitivity in y-direction (pc/psi)	23,200	6,900	4,100	3,700	3,200
Nonlinearity in x of full scale (%)	~0	~0	~0	~0	4.25
Nonlinearity in y of full scale (%)	0.25	5.84	6	~ 4.6	3.5
Repeatability in x of reading (%)	1	1	1	1	1
Repeatibility in y of reading (%)	1	1	1	1	1
Signal to acceleration ratio, x	100:1	90:1	100:1	90:1	80:1
Signal to acceleration ratio, y	80:1	80:1	80:1	80:1	70:1
Signal to 3rd axis input (1 psi)					
x (pc)	3	~ 0	~0	~0	~0
y (pc)	10	~ 0	~0	~0	~0
1st order interaction in x of reading (%)	0.39	3.84	1.68	1.56	1.27
1st order interaction, y (%)	0.323	0.42	2.13	2.00	1.9
2nd order interaction, x (%)	0.122	2.38	1.1	1.00	3.54
2nd order interaction, y (%)	0.198	7.5	1.87	1.50	3.95
Temperature dependency, % of 25°C sensitivity					
x, 50°C	4.8	4	3	4	4.5
y, 70°C	5.3	4.7	5	5	5
x, 50°C	6.4	5.2	4.2	4.2	5.8
y, 70°C	7.5	7.3	5	6	7.4
Natural frequency in H_z					
x	3,600	5,000	5,000	5,800	7,500
y	1,780	3,300	4,150	4,200	5,000

Bottom view of transducers

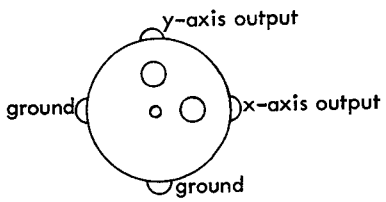

CONCLUSIONS AND REMARKS

Five piezoelectric surface shear force transducers have been constructed and delivered to IRD, LRC, NASA. These transducers satisfy the prescribed specifications. This report has described the analysis, construction and calibration of the transducer.

Transducers of this kind require high sensitivity, mechanical rigidity, high temperature operation, smallness in size, high natural frequency, flat dynamic response, and low acceleration sensitivity. These characteristics can be easily obtained from a monolithic silicon integrated sensor. The advent of integrated circuitry made this possible recently.